

# A JOINT DETECTION AND RECONSTRUCTION METHOD FOR BLIND GRAPH SIGNAL RECOVERY

Xianghui Mao and Yuantao Gu

Department of Electronic Engineering, Tsinghua University, Beijing 100084, China.

## ABSTRACT

Sampling and reconstruction is a fundamentally important problem in the field of graph signal processing. Many works have been contributed to reconstructing bandlimited signals from measurements taken on a known subset of vertices. However, in some cases, the vertex defects occur randomly over the graph. In such situation, the existing graph signal reconstruction methods fail to deal with such blind reconstruction problem. In this paper, we formulate the blind reconstruction problem as Mixed-Integer Nonlinear Programming, and propose a Joint Detection and Reconstruction (JDR) method to simultaneously detect the vertices' working states and reconstruct the bandlimited signal. The convergence property of the proposed method is analyzed. In the experimental part, both synthetic dataset and real-world dataset are applied to verify the proposed methods.

**Index Terms**— blind reconstruction, bandlimited graph signal, mixed-integer nonlinear programming.

## 1. INTRODUCTION

As a fundamental problem in signal processing, graph signal sampling and reconstruction is widely studied. Aimed at preserving sufficient information of bandlimited graph signals for reconstruction, sampling schemes including determinant selection sampling [1, 2, 3], random selection sampling [4], local measurement based sampling [5], and aggregation sampling [6] have been proposed.

When a bandlimited signal  $\mathbf{x}$  over an  $N$ -vertex graph is sampled according to the selection sampling scheme, the operation is modeled as the following:

$$\mathbf{y} = \mathbf{h} \circ \mathbf{x} + \mathbf{n}, \quad \mathbf{h} \in \{0, 1\}^N, \quad (1)$$

where the vector  $\mathbf{h} = [h_1, \dots, h_N]^T$  collects the boolean working states of the vertices, where  $h_i$  equal 1 when vertex  $v_i$  works and 0 for  $v_i$  being defective,  $\circ$  denotes the Hadamard product, and  $\mathbf{n} \sim \mathcal{N}(\mathbf{0}_N, \sigma^2 \mathbf{I}_N)$  represents the additive Gaussian white noise. Some existing works [2, 7, 8] discuss the theoretical conditions for the exact reconstruction of bandlimited signals from noiseless observations. A sampling set is called uniqueness set if bandlimited graph signals can be uniquely determined by the sampled entries [7].

With the sampling states vector  $\mathbf{h}$  well-designed and known as a priori, many bandlimited graph signal reconstruction methods have been proposed, including least square approach [9], iterative

least square method [10], iterative weighting method and iterative propagating methods [3], diffusion operator based method [11], and kernel-based reconstruction [12], etc.

However, in some cases, due to random vertex defects, the sampling set can not be artificially designed, and the entries of graph signals observed is not artificially designed but randomly formed with the sampling states of  $\mathbf{h}$  blind to the reconstruction method. Specifically, it is unknown which vertices carry information about the original signal, and which return pure noise. In such situation, reconstructing  $\mathbf{x}$  from  $\mathbf{y}$  becomes a more difficult problem, and beyond the scope of the existing graph signal reconstruction methods.

We noticed that a special case that  $\mathbf{x}$  is of constant value, or equivalently,  $\mathbf{x}$  is 0-bandlimited, is dealt with in [13]. However, to the best of our knowledge, no prior work has been presented tackling the blind reconstruction of general bandlimited graph signals. Within a broader range of blind processing of graph signals, [14] proposed a method to trace back the sparse input to the graph by the technique of blind deconvolution. In this paper, we address this problem for the first time and propose a Joint Detection and Reconstruction (JDR) method to simultaneously detect the working states of the vertices and reconstruct the bandlimited graph signal. Theoretical analysis and experimental validation are also included to demonstrate the behavior of the proposed method.

## 2. PRELIMINARIES

Provided an  $N$ -vertex undirected weighted graph  $\mathcal{G}$ , a graph signal  $\mathbf{x}$  is an  $N$ -dimensional vector, with the  $i$ th element  $x_i$  denotes the scalar assigned to the vertex  $v_i$ . To analyze the spectral characteristics of graph signals, graph Fourier transform is introduced via the graph Laplacian  $\mathbf{L} = \mathbf{D} - \mathbf{A}$ , with  $\mathbf{A} \in \mathbb{R}^{N \times N}$  denoting the adjacency matrix, and diagonal matrix  $\mathbf{D} = \text{diag}(d_1, \dots, d_N)$  collecting the degrees of vertices as its diagonal entries.  $\mathbf{L}$  is a semi-definite symmetric matrix, with eigenvalues  $0 = s_1 \leq \dots \leq s_N$  indicating the frequencies of  $\mathcal{G}$ , and the corresponding eigenvectors,  $\mathbf{u}_1, \dots, \mathbf{u}_N$ , constitute the graph Fourier basis. Then the frequency component of signal  $\mathbf{x}$  on the frequency point  $s_k$  is denoted as  $\tilde{x}_k = \mathbf{u}_k^T \mathbf{x}$ . For detailed discussion on graph Fourier transform, the readers may refer to [15].

A graph signal  $\mathbf{x}$  is called  $\omega$ -bandlimited if the spectral support of  $\mathbf{x}$  is in the range of  $[0, \omega]$ . All the  $\omega$ -bandlimited signals on graph  $\mathcal{G}$  constitute a Hilbert subspace named Paley-Wiener space, denoted as  $PW_\omega(\mathcal{G})$ . For any graph signal  $\mathbf{x} \in PW_\omega(\mathcal{G})$ , there is  $\tilde{x}_k = 0, \forall k \in \{j : s_j > \omega\}$ . Intuitively, the bandlimited signals exhibit smoothness with respect to the corresponding graph topology.

## 3. PROBLEM MODELING

We consider the case that the vertex defects occur independently among the vertices, and the defect probability of each vertex is a

The authors are with the Department of Electronic Engineering, Tsinghua University, Beijing 100084, China. This work was partially supported by National Natural Science Foundation of China (NSFC 61571263, 61531166005), the National Key Research and Development Program of China (Project No. 2016YFE0201900, 2017YFC0403600), and Tsinghua University Initiative Scientific Research Program (Grant 2014Z01005). The corresponding author of this work is Y. Gu (E-mail: gyt@tsinghua.edu.cn).

prior knowledge stacked in vector  $\mathbf{p} = [p_1, \dots, p_N]^T \in [0, 1]^N$ . Specifically, with probability  $p_i$ , the vertex  $v_i$  is defective, and with probability  $1 - p_i$ , the vertex  $v_i$  works. Whether a vertex works is not influenced by the working states of other vertices. Recalling the observing model (1), we have that the working state of vertex  $v_i$  decides whether the observation  $y_i$  is pure noise or signal value  $x_i$  with additive noise.

In such scenario, we propose to jointly detect the working state vector  $\mathbf{h}$  and reconstruct the bandlimited graph signal  $\mathbf{x}$  according to the Maximum a posteriori (MAP) criterion. Concretely speaking, the problem could be casted as the following.

$$\begin{aligned} \max_{\mathbf{h}, \mathbf{x}} P(\mathbf{h}|\mathbf{y}; \mathbf{x}) &\propto P(\mathbf{y}|\mathbf{h}; \mathbf{x})P(\mathbf{h}), \\ \text{s.t. } \mathbf{h} &\in \{0, 1\}^N, \mathbf{x} \in PW_\omega(\mathcal{G}). \end{aligned} \quad (2)$$

According to the observing model illustrated in (1), with  $\mathbf{h}$  and  $\mathbf{x}$  given, the observations at different vertices, i.e.  $y_1, \dots, y_N$ , are independent from each other. In addition, the prior information on  $\mathbf{h}$  implies that the prior distribution of the vertices' working states are mutually independent. Or equivalently, we have

$$P(\mathbf{y}|\mathbf{h}; \mathbf{x}) = \prod_{i=1}^N P(y_i|h_i; x_i), \quad P(\mathbf{h}) = \prod_{i=1}^N P(h_i). \quad (3)$$

Specifically, the posterior probability of random variable  $h_i$  is proportional to (4).

$$\begin{aligned} &P(y_i|h_i; x_i)P(h_i) \\ &\propto (h_i(1 - p_i) + (1 - h_i)p_i) \exp\left(-\frac{(y_i - h_i x_i)^2}{2\sigma^2}\right), \\ &\propto \exp\left(-w_i h_i - \frac{(y_i - h_i x_i)^2}{2\sigma^2}\right), \end{aligned} \quad (4)$$

where  $w_i := \ln \frac{p_i}{1-p_i}$  is introduced to put the prior information on  $h_i$  into the exponent.

According to (3) and (4), problem (2) could be put into the following equivalent form as shown in (5).

$$\begin{aligned} \min_{\mathbf{h}, \mathbf{x}} \mathbf{w}^T \mathbf{h} + \frac{\|\mathbf{y} - \mathbf{h} \circ \mathbf{x}\|_2^2}{2\sigma^2}, \\ \text{s.t. } \mathbf{x} \in PW_\omega(\mathcal{G}), \mathbf{h} \in \{0, 1\}^N, \end{aligned} \quad (5)$$

where  $\mathbf{w} = [w_1, w_2, \dots, w_N]^T$ . But notice that the working vertices do not necessarily constitute a uniqueness set. In other words, even the vertices' working states vector  $\mathbf{h}$  is correctly detected by solving (5), the corresponding optimal bandlimited graph signal  $\mathbf{x}$  is not unique. To get rid off such multiple reconstructed signals case, we target on reconstructing the possible bandlimited signals with small energy by solving (6) instead of (5).

$$\begin{aligned} \min_{\mathbf{h}, \mathbf{x}} \mathbf{w}^T \mathbf{h} + \frac{\|\mathbf{y} - \mathbf{h} \circ \mathbf{x}\|_2^2}{2\sigma^2} + \lambda \|\mathbf{x}\|_2^2 =: F(\mathbf{x}, \mathbf{h}), \\ \text{s.t. } \mathbf{x} \in PW_\omega(\mathcal{G}), \mathbf{h} \in \{0, 1\}^N, \end{aligned} \quad (6)$$

where the parameter  $\lambda > 0$  is introduced to induce the uniqueness of reconstructed signal. To be noted, the unique optimal  $\mathbf{x}$  to problem (6) is not guaranteed to be the original signal. Specifically, when the restored working states do not compose a uniqueness set, the reconstructed  $\mathbf{x}$  is not trustable. We will discuss the trustability of the reconstruction result in the next section.

With  $\mathbf{w} = \mathbf{0}_N$ , the above MAP estimator (6) is transformed into a Maximum likelihood (ML) estimator, which fits for the scenario where prior distribution parameter  $\mathbf{p}$  is not available.

**Table 1.** Joint Detection and Reconstruction (JDR) Framework

---

<b>Input:</b> observations $\mathbf{y}$ , detection function $D(\cdot, \cdot)$ ,
reconstruction function $R(\cdot, \cdot)$ , maximum iteration $K$ , threshold $\varepsilon$ .
<b>Output:</b> detected working state $\hat{\mathbf{h}}$ , reconstructed signal $\hat{\mathbf{x}}$ .
<b>Initialization:</b> $\mathbf{x}^0 = \mathbf{y}$ , $k = 0$ ;
<b>Repeat:</b>
1) Detect defects $\mathbf{h}^{k+1} = D(\mathbf{x}^k, \mathbf{y})$ ;
2) Reconstruct graph signal $\mathbf{x}^{k+1} = R(\mathbf{h}^{k+1}, \mathbf{y})$ ;
3) $(\hat{\mathbf{h}}, \hat{\mathbf{x}}) = (\mathbf{h}^k, \mathbf{x}^k)$ , $k = k + 1$ ;
<b>Until:</b> $k = K$ or $ F(\mathbf{x}^k, \mathbf{h}^k) - F(\mathbf{x}^{k+1}, \mathbf{h}^{k+1})  < \varepsilon$ .

---

## 4. JOINT DETECTION AND RECONSTRUCTION METHOD

The core problem we aim to solve, (6), is a nonconvex Mixed-Integer Nonlinear Programming (MINLP) problem, which makes it hard to solve [16]. Noticing that both the nonlinearity and nonconvexity comes from the term  $\|\mathbf{y} - \mathbf{h} \circ \mathbf{x}\|_2^2$ , we find the blessing of such formulation is that when the integer decision variable  $\mathbf{h}$  is continuous, i.e.,  $\mathbf{h} \in [0, 1]^N$ , problem (6) turns into a biconvex optimization problem. If the optimization variables are continuous, the alternative updating method is prevalently applied to solve biconvex optimization problem [17].

In light of this idea, we propose to use this alternative updating rule to solve the original MINLP problem (6). That is, alternatively fixing one and updating the other, but one of them is constrained to be an integer. We can simply accomplish this by limiting the searching domain of  $\mathbf{h}$  to be discrete.

The updating framework is given in Table 1. The explicit definition of the detection function  $D(\cdot, \cdot)$  and reconstruction function  $R(\cdot, \cdot)$  are as follows:

$$D(\mathbf{x}, \mathbf{y}) = \underset{\mathbf{h}}{\operatorname{argmin}} F(\mathbf{x}, \mathbf{h}), \text{ s.t. } \mathbf{h} \in \{0, 1\}^N, \quad (7)$$

$$R(\mathbf{h}, \mathbf{y}) = \underset{\mathbf{x}}{\operatorname{argmin}} F(\mathbf{x}, \mathbf{h}), \text{ s.t. } \mathbf{x} \in PW_\omega(\mathcal{G}). \quad (8)$$

### 4.1. Detection Function $D(\cdot, \cdot)$

A direct observation is that the optimization problem (7) is fully separable over the vertices. Hence, we have  $D(\mathbf{x}, \mathbf{y}) = [D_1(x_1, y_1), \dots, D_N(x_N, y_N)]^T$ , with each element

$$D_i(x_i, y_i) = \underset{h_i \in \{0, 1\}}{\operatorname{argmin}} w_i h_i + \frac{(y_i - h_i x_i)^2}{2\sigma^2}, \quad (9)$$

$$= \begin{cases} 1, & (x_i)^2 - 2x_i y_i < -2\sigma^2 w_i; \\ 0, & \text{elsewhere.} \end{cases} \quad (10)$$

### 4.2. Reconstruction Function $R(\cdot, \cdot)$

The reconstructing function  $R(\cdot, \cdot)$  admits a closed-form formulation, that is,  $R(\mathbf{h}, \mathbf{y}) = \mathbf{U}_\omega \mathbf{Q}^{-1} \mathbf{U}_\omega^T \operatorname{diag}(\mathbf{h}) \mathbf{y}$ , where  $\mathbf{Q} = \mathbf{U}_\omega^T \operatorname{diag}(\mathbf{h}) \mathbf{U}_\omega + 2\sigma^2 \lambda \mathbf{I}_N$ . Noticing that  $\mathbf{Q}$  is positive definite, function  $R(\mathbf{h}, \mathbf{y})$  is well defined.

In addition, as the added regularization term is convex and differentiable, many existing iterative bandlimited graph signal reconstruction methods, including [10] and [3], could be readily generalized to approximate  $R(\cdot, \cdot)$ . By implementing the iterative method, a nearly optimal result to problem (8) can be achieved without calculating the matrix inversion. Considering that the computational complexity is not among the main concerns of this work, detailed discussion on iterative methods is omitted here.

### 4.3. Trustability of Reconstruction Result

As mentioned in the previous section, even when the working states vector  $\mathbf{h}$  is correctly detected, sometimes the reconstructed graph signal is trustable due to the less of samples. As is known, the invertibility of the matrix  $\mathbf{U}_\omega^T \text{diag}(\mathbf{h}) \mathbf{U}_\omega$  implies that the working vertices labeled by the 1's in  $\mathbf{h}$  forms a uniqueness set. Furthermore, when the working vertices do form a uniqueness set, the condition number of this matrix is positively correlated with the condition number of matrix  $\mathbf{Q}$ . The condition number of  $\mathbf{Q}$  evaluates the stability of the reconstructed result. That is, with a larger condition number, the reconstructed result is less stable to perturbation on the observation  $\mathbf{y}$ . So we evaluate the trustability of the reconstruction result by the condition number of  $\mathbf{U}_\omega^T \text{diag}(\mathbf{h}) \mathbf{U}_\omega$ . Specifically, if the condition number is close to 1, we claim that the reconstruction result being trustable; otherwise, if it tends to infinity, we do not trust the reconstruction result.

## 5. SOLVER ANALYSIS

As an extension of alternative solver to biconvex minimization problems, we find that the proposed alternative solver to problem (6) share some nice properties. The readers may refer to [17] for a detailed theoretical analysis on biconvex minimization problem. In this section, we present theoretical analysis to the proposed JDR method by extending part of the results on biconvex minimization problem to the scenario of biconvex MINLP.

**Remark 1.** *The sequence of objective function value  $\{F(\mathbf{h}^k, \mathbf{x}^k)\}_{k \in \mathbb{N}}$  converges monotonically to a  $F^*$ .*

*Proof.* According to the definition of  $D(\cdot, \cdot)$  and  $R(\cdot, \cdot)$  given in (7) and (8), we have

$$F(\mathbf{h}^{k+1}, \mathbf{x}^{k+1}) \leq F(\mathbf{h}^{k+1}, \mathbf{x}^k) \leq F(\mathbf{h}^k, \mathbf{x}^k). \quad (11)$$

In other words,  $\{F(\mathbf{h}^k, \mathbf{x}^k)\}_{k \in \mathbb{N}}$  is a decreasing sequence. Further considering that the function  $F(\cdot, \cdot)$  is lower bonded by  $\sum_{i: p_i < 1/2} w_i$ , the assertion in Remark 1 is achieved.  $\square$

**Remark 2.** *The sequence of variables  $\{\mathbf{h}^k\}_{k \in \mathbb{N}}$  satisfies the following properties:*

- *there is at least one accumulation point  $(\mathbf{h}^*, R(\mathbf{h}^*, \mathbf{y}))$  of the sequence;*
- *each accumulation point is a feasible solution to problem (6) with the same objective function value  $F^*$ .*

*Proof.* First, the feasible set of variable  $\mathbf{h}$ ,  $\{0, 1\}^N$ , is a compact set. Second, thanks to the introduced positive parameter  $\lambda$ , for any  $1 \leq k \leq K$ , the reconstructed signal in the  $k$ th iterate,  $\mathbf{x}^k$ , is uniquely decided by the detection result  $\mathbf{h}^k$  with  $\mathbf{x}^k = R(\mathbf{h}^k, \mathbf{y})$ . Hence, we have that the detection vector sequence  $\{\mathbf{h}^k, \mathbf{x}^k\}_{k \in \mathbb{N}}$  has at least one accumulation point. Consequently, there is at least one accumulation point  $(\mathbf{h}^*, R(\mathbf{h}^*, \mathbf{y}))$  of the sequence  $\{(\mathbf{h}^k, \mathbf{x}^k)\}_{k \in \mathbb{N}}$ .

With the above analysis, we have a subsequence  $\{\mathbf{h}^k\}_{k \in \mathcal{K}}$  converging to  $\mathbf{h}^*$ . Provided that the feasible set of  $\mathbf{h}$  is discrete, a fact is that there exists a number  $n$ , for any  $k \in \mathcal{K}$  that is greater than  $n$ , we have  $(\mathbf{h}^k, \mathbf{x}^k) = (\mathbf{h}^*, R(\mathbf{h}^*, \mathbf{y}))$ . The feasibility of  $(\mathbf{h}^k, \mathbf{x}^k)$ ,  $\forall k > 1$  is straightforward from the definition of  $R(\cdot, \cdot)$  and  $D(\cdot, \cdot)$ . Recalling Remark 1, a direct result is  $F(\mathbf{h}^*, R(\mathbf{h}^*, \mathbf{y})) = F^*$ .  $\square$

Remark 1 indicates that with more iterations conducted, we can always expect a better detection and reconstruction result under the criterion of minimizing function  $F$ . With Remark 1 discussing the function value, Remark 2 gives a hint on the detection and reconstruction result, that is, when sufficiently many iterations are performed, the achieved detection and reconstruction result is an accumulation point. In other words, if we continue iterating without stopping, the same solution will appear infinitely many times. However, the uniqueness and convergence analysis of the detection and reconstruction result are still open problems.

## 6. EXPERIMENTAL RESULTS

We validate the proposed JDR method with both synthetic dataset and real-world dataset. Based on the synthetic dataset, the robustness of the proposed method is tested under different settings. Experiments with the temperature dataset further demonstrates the performance with the defect probabilities  $\mathbf{p}$  known or unknown.

### 6.1. Synthetic Dataset

To generate the synthetic dataset, we randomly locate  $N = 100$  vertices according to the uniform distribution within the square  $[0, 1] \times [0, 1]$ . A graph is achieved by applying the  $k$ -nearest neighbor ( $k$ -nn) method with  $k = 5$ . The  $\omega$ -bandlimited signals  $\mathbf{x}$  are normalized isotropically distributed random vectors residing in  $PW_\omega(\mathcal{G})$ . The working states of the vertices are randomly generated with the same defect probabilities  $p_i$ . The observation  $\mathbf{y}$  is achieved by (1). The experimental results are the average of 5E4 independent trials.

In the first experiment, we demonstrate how the defect probability and signal bandwidth affect the detection and reconstruction performance. The signal-to-noise ratio (SNR) is 20dB. One can read from the left plot of Fig. 1 that for various bandwidths, the detection error first increases then decreases as  $p_i$  goes up, and the peak appears at  $p_i = 0.5$ . The reason is that when  $p_i$  equals 0.5, the entropy of  $\mathbf{h}$  approaches its maximum, or equivalently, the vertices' working states are the most uncertain. One may further notice that the detection error curve is not symmetric about  $p_i = 0.5$ . With  $p_i$  increasing over 0.5 towards 1, the corresponding detection error at  $p_i$  is larger than that at  $1 - p_i$ . This observation coincides with the increasing pattern of the condition number curves and the signal reconstruction error curves as shown in right two plots of Fig. 1. The reason is that with  $p_i$  growing towards 1, more defects occur, and less information of the original signal is available, leading to the sharp increase of the condition number, and hence the increase of reconstruction error, further preventing the rapid decrease of the detection error. This phenomenon also implies that the condition number is a good criterion to evaluate the trustability of the reconstruction result. As to the bandwidth, when  $\omega$  increases, more working vertices are required to achieve a trustable reconstruction or a same signal reconstruction quality.

In the second experiment, the proposed JDR method is tested in different noise scenarios and the performance is demonstrated in Fig. 2. Comparing different SNR settings, the curves in each subplot of Fig. 2 follow the same trend when  $p_i$  varies. And better detection

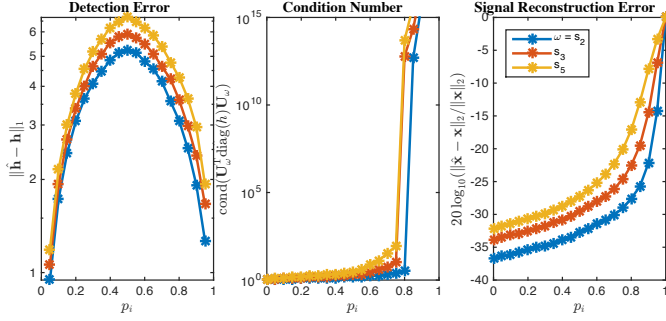


**Fig. 1.** The performance of the proposed JDR method with various defect probability and cut-off frequency.

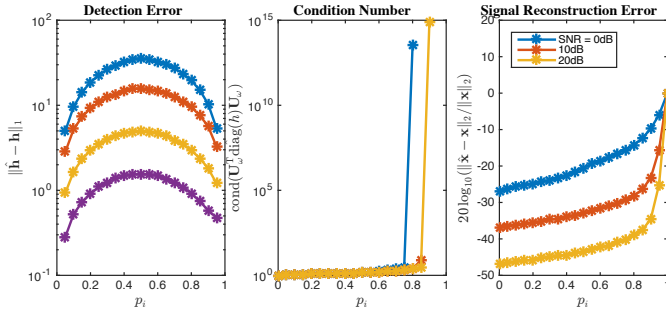


**Fig. 2.** The performance of the proposed JDR method with various defect probability and SNR.

and reconstruction performance is achieved under high SNR setting. Besides, the right subplot of Fig. 2 indicates that when the defect probability is rather small (below 0.1), a more than 15dB SNR gain is achieved by applying the proposed method.

## 6.2. Temperature Dataset

To evaluate the performance of the proposed JDR method on real-world data, we experiment with the temperature dataset [18] collected by 150 weather stations located in the mainland of America over the year of 2015. Taking each station as a vertex, a graph is formed by applying 8-nn method. The edge weight is taken as the inverse of the square geodesic distance between the connected stations. A graph signal  $\mathbf{x}$  corresponds to the temperature at all stations at a single day. Fig. 3 displays one of the 365 graph signals and one can observe that it is smooth with respect to the generated graph, and could be approximated by bandlimited graph signals. Hence, we project the graph signals onto the subspace  $PW_{s_{10}}(\mathcal{G})$  to obtain  $s_{10}$ -bandlimited graph signals. With  $p_1 = \dots = p_N$ , observations of each temperature are obtained according to the observing model (1) with the SNR fixed as 20dB.

In this experiment, we test the proposed method in two different scenarios, i.e., with the defect probability  $p_i$  known and unknown, respectively. As discussed in section III, while  $p_i$  is unknown, an ML estimator is applied by setting  $\mathbf{w} = \mathbf{0}_N$ . By varying the defect probability  $p_i$  from 0 to 1, the detection and reconstruction errors are compared in Fig. 4. As a reference, the curve with legend “h known” is achieved by reconstructing  $\mathbf{x}$  via calculating  $R(\mathbf{h}, \mathbf{y})$ .

On the one hand, it can be read from Fig. 4 that the trends of all 3 types of curves produced by the MAP-based method are in

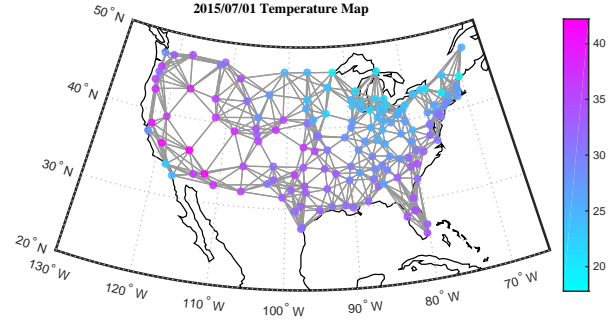


**Fig. 3.** The graph topology is displayed and a graph signal composed of temperatures ( $^{\circ}C$ ) at July 1st, 2015 is visualized by color.

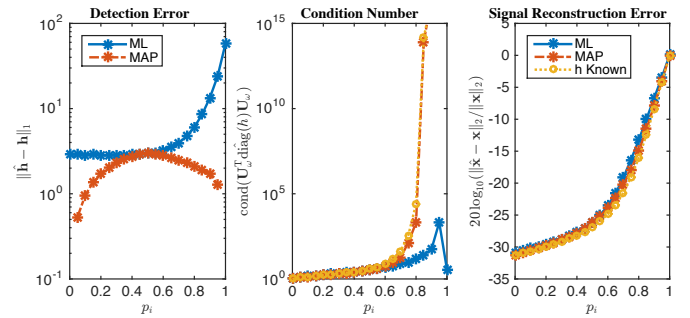


**Fig. 4.** The performance of the proposed JDR with different defect probability. Each point is averaged over 365 signals, each observed 50 times.

good consistency with those shown in Fig. 1 and 2. On the other hand, the detection error curve given by the ML-based method is flat before a quick increase, where the increase coincides with the increase of the reconstruction error. And the inadequacy of the working vertices is the main driven factor of such increase. Comparing the two solvers, as more prior information is utilized, MAP-based method delivers better detection and reconstruction results than the ML-based method. In the middle plot, when  $p_i$  approaches 1, the ML-based method gives detection result with low condition number, but the amount of samples is not adequate to reconstruct the original graph signal, and hence the reconstruction result is not trustable due to the high detection error, which further implies that the condition number can only evaluate the trustability of the reconstruction result given by MAP-based method but not for ML-based method. In addition, the signal reconstruction error given by the two proposed methods are close to the reconstruction error when working state vector  $\mathbf{h}$  is aware.

## 7. CONCLUSION

This paper studies the problem of blind reconstruction of bandlimited graph signal, which is formulated as an MINLP problem for the first time. We then propose a joint detection and reconstruction method to simultaneously detect the working states of the vertices and reconstruct the graph signal. Experiments on both synthetic dataset and real-world dataset verify the proposed method in solving blind reconstruction problem.

## 8. REFERENCES

- [1] Isaac Pesenson, "Sampling in Paley-Wiener spaces on combinatorial graphs," *Transactions of the American Mathematical Society*, vol. 360, no. 10, pp. 5603–5627, 2008.
- [2] Siheng Chen, Rohan Varma, Aliaksei Sandryhaila, and Jelena Kovačević, "Discrete signal processing on graphs: Sampling theory," *IEEE Transactions on Signal Processing*, vol. 63, no. 24, pp. 6510–6523, 2015.
- [3] Xiaohan Wang, Pengfei Liu, and Yuantao Gu, "Local-set-based graph signal reconstruction," *IEEE Transactions on Signal Processing*, vol. 63, no. 9, pp. 2432–2444, 2015.
- [4] Gilles Puy, Nicolas Tremblay, Rémi Gribonval, and Pierre Vandergheynst, "Random sampling of bandlimited signals on graphs," *Applied and Computational Harmonic Analysis*, 2016.
- [5] Xiaohan Wang, Jiaxuan Chen, and Yuantao Gu, "Local measurement and reconstruction for noisy bandlimited graph signals," *Signal Processing*, vol. 129, pp. 119–129, 2016.
- [6] Antonio G Marques, Santiago Segarra, Geert Leus, and Alejandro Ribeiro, "Sampling of graph signals with successive local aggregations," *IEEE Transactions on Signal Processing*, vol. 64, no. 7, pp. 1832–1843, 2016.
- [7] Aamir Anis, Akshay Gadde, and Antonio Ortega, "Towards a sampling theorem for signals on arbitrary graphs," in *Acoustics, Speech and Signal Processing (ICASSP), 2014 IEEE International Conference on*. IEEE, 2014, pp. 3864–3868.
- [8] Mikhail Tsitsvero, Sergio Barbarossa, and Paolo Di Lorenzo, "Signals on graphs: Uncertainty principle and sampling," *IEEE Transactions on Signal Processing*, vol. 64, no. 18, pp. 4845–4860, 2016.
- [9] Sunil K Narang, Akshay Gadde, and Antonio Ortega, "Signal processing techniques for interpolation in graph structured data," in *Acoustics, Speech and Signal Processing (ICASSP), 2013 IEEE International Conference on*. IEEE, 2013, pp. 5445–5449.
- [10] Sunil K Narang, Akshay Gadde, Eduard Sanou, and Antonio Ortega, "Localized iterative methods for interpolation in graph structured data," in *Global Conference on Signal and Information Processing (GlobalSIP), 2013 IEEE*. IEEE, 2013, pp. 491–494.
- [11] Lishan Yang, Kangyong You, and Wenbin Guo, "Bandlimited graph signal reconstruction by diffusion operator," *EURASIP Journal on Advances in Signal Processing*, vol. 2016, no. 1, pp. 120, 2016.
- [12] Daniel Romero, Meng Ma, and Georgios B Giannakis, "Kernel-based reconstruction of graph signals," *IEEE Transactions on Signal Processing*, vol. 65, no. 3, pp. 764–778, 2017.
- [13] Qing Zhou, Di Li, Soumya Kar, Lauren M Huie, H Vincent Poor, and Shuguang Cui, "Learning-based distributed detection-estimation in sensor networks with unknown sensor defects," *IEEE Transactions on Signal Processing*, vol. 65, no. 1, pp. 130–145.
- [14] David Ramírez, Antonio G Marques, and Santiago Segarra, "Graph-signal reconstruction and blind deconvolution for diffused sparse inputs," in *Acoustics, Speech and Signal Processing (ICASSP), 2017 IEEE International Conference on*. IEEE, 2017, pp. 4104–4108.
- [15] David I Shuman, Sunil K Narang, Pascal Frossard, Antonio Ortega, and Pierre Vandergheynst, "The emerging field of signal processing on graphs: Extending high-dimensional data analysis to networks and other irregular domains," *IEEE Signal Processing Magazine*, vol. 30, no. 3, pp. 83–98, 2013.
- [16] Pietro Belotti, Christian Kirches, Sven Leyffer, Jeff Linderoth, James Luedtke, and Ashutosh Mahajan, "Mixed-integer nonlinear optimization," *Acta Numerica*, vol. 22, pp. 1–131, 2013.
- [17] Jochen Gorski, Frank Pfeuffer, and Kathrin Klamroth, "Biconvex sets and optimization with biconvex functions: a survey and extensions," *Mathematical Methods of Operations Research*, vol. 66, no. 3, pp. 373–407, 2007.
- [18] "Global historical climatology network - daily (ghcnd)," <http://www.ncdc.noaa.gov/data-access/land-based-station-data>.